DOI: https://doi.org/10.31351/vol35iss1pp243-261

The Effectiveness of Topical Nanohydrogel Pegagan Leaf Extract in Healing of Excision Wounds in Hyperglycemic Wistar Rats

Muhammad Hafizh Abiyyu Fathin Fawwazi[1], Farida Hayati[*,2], Lutfi Chabib[2] and Tedi Rustandi[1]

[1]Department of Pharmacy, Sekolah Tinggi Ilmu Kesehatan ISFI Banjarmasin, Banjarmasin, Indonesia.
[2]Department of Pharmacy, Faculty of Mathematics and Natural Sciences, Universitas Islam Indonesia, Yogyakarta, Indonesia.
***Corresponding author**
Received 1/2/2025, Accepted 7/8/2025, Published 29/3/2026

Abstract

Individuals with diabetes are susceptible to complications from diabetic foot ulcers, making it crucial to explore natural product-based dosage forms as alternative treatments for diabetic wound healing. One such natural product is the *Centella asiatica* (L.) plant, known to contain asiatic acid compounds that promote wound healing. However, these compounds exhibit low bioavailability. This study aims to evaluate the wound healing effectiveness of a topical nanohydrogel of *C. asiatica* leaf extract in hyperglycemic rats. *C. asiatica* leaves were extracted with 96% ethanol for 72 hours and formulated into a nanohydrogel. The diabetes was induced with a single dose of nicotinamide 230 mg/kgBW 15 minutes before the induction of streptozotocin 65 mg/kgBW intraperitoneally. Two excision wounds on the back of the rat with a diameter of 6 mm. Treatment was carried out for 14 days and macroscopic observations. At the end of the study, histopathological examination was performed on skin samples and wound healing percentages were analyzed using One-way ANOVA. Molecular docking studies were carried out on the target receptors S. aureus, mitogen-activated protein kinase 3 (MAPK3), Nuclear Factor-κB (NF-κB), and the IL-6/IL-6Rα/IL-6Rβ complex. Formula 1 nanoemulsion matrix is an optimum matrix with a particle size of 20.3 ± 0.3 nm, PI 0.414 ± 0.203, zeta potential -31.0 ± 0.7, percent transmittance 89.507 ± 0.0, and particle size <50nm, as shown by TEM. Nanohydrogel 1% significantly accelerated diabetic wound healing compared to the negative control ($p<0.05$). Histological examination revealed that wounds treated with 1% nanohydrogel had a moderate collagen composition and were rich in macrophages, which are beneficial in wound healing. Asiatic acid has an affinity level of -8.4 kcal/mol (S. aureus), -8.3 kcal/mol (MAPK3), -6.9 kcal/mol (NF-κB), and -8.5 kcal/mol (IL-6/IL-6Rα/IL-6Rβ complex). Nanohydrogel 1% is biocompatible and accelerates wound healing in hyperglycemic rats.
Keywords: Asiatic acid, *Centella asiatica*, Diabetic wound healing, Molecular docking, Nanohydrogel.

Introduction

Diabetes Mellitus (DM) remains one of the most prevalent degenerative diseases in Indonesia. According to the International Diabetes Federation (IDF) data from 2021, an estimated 19.465 million people in Indonesia have diabetes, while globally, 537 million people are affected[(1)]. Diabetes patients often experience complications, one of which is diabetic foot ulcers, which have a global prevalence of 3-13%, with 15-20% resulting in amputation[(2,3)].

Despite various efforts to develop treatments for diabetic ulcers, the results have not been optimal. Current methods, such as the use of synthetic chemical drugs and physical treatments, are often ineffective and come with high economic costs[(4,5)]. Moreover, diabetic foot ulcers can progress to diabetic ulcer infections, closely linked to antibiotic resistance due to the widespread use of antibiotics[(6)]. Therefore, it is crucial to explore effective and optimal therapeutic approaches for diabetic foot ulcers, including the use of active compounds derived from plants[(7)].

One plant with potential as an alternative treatment for diabetic foot ulcers is *Centella asiatica* (L.) (Pegagan), a native Indonesian herb traditionally used as a medicinal plant. *Centella asiatica* is reported to contain triterpenoid compounds (madecassoside, asiaticoside, madecassic acid, and asiatic acid) responsible for antimicrobial, anticancer, neuroprotective, immunomodulatory, anti-inflammatory, antioxidant, hepatoprotective, and wound healing activities[(8–10)].

Asiatic acid, in particular, has been reported to be the most effective compound for wound healing. However, asiatic acid is poorly soluble in water, with a concentration in saturated saline of only 0.1583 mg/ml, leading to low bioavailability and reduced effectiveness in wound healing[11]. To address the low bioavailability of asiatic acid, it is necessary to develop a topical formulation that can enhance the bioavailability and effectiveness of the compounds in *Centella asiatica* extract. Nanohydrogels are one such topical formulation that can increase bioavailability and reduce compound size (20-200 nm), potentially enhancing therapeutic efficacy[12]. Additionally, nanohydrogels are favored by the public due to their cooling sensation on the skin[13].Research on wound healing effectiveness has been extensively conducted, including studies using hyperglycemic/diabetic-induced rats as test animals[14]. Rats are chosen as test animals due to several advantages: they are easy to handle, cost-effective, have low mortality rates, and share pathological and metabolic similarities with humans[15]. Rats exhibit a primary wound healing mechanism through rapid contraction, aided by the panniculus carnosus muscle, which accelerates collagen formation and remodeling processes, occurring earlier than in humans, approximately within six days[16]. Given the reported activity and bioactive compound content in *Centella asiatica*, developing a topical nanohydrogel formulation of *Centella asiatica* leaf extract as an alternative agent for diabetic wound healing is highly feasible.

Materials and Methods

Materials

C. asiatica leaves collected from Kalibawang, Kulonprogo, Yogyakarta and had been determinated from Systematics Laboratory, Faculty of Biology, Universitas Gadjah Mada with certificate number 0141085/S.Tb./IX/2021. Aquadest, Ethanol 70%, Ethanol 96%, Tween 80, Propylene glycol, Propyl Paraben, Methyl paraben were purchased from PT. Brataco (Yogyakarta, Indonesia), Streptozotocin (Sigma-Aldrich), Carbopol-940 (Sigma-Aldrich), Isopropyl myristate (Merck), Nicotinamide (Merck), Ketamine (Ilium), Xylazine (Holland). Male Wistar rats obtained from Laboratorium Penelitian dan Pengujian Terpadu (LPPT), Universitas Gadjah Mada.

Ethical Clearance

This study has been approved by the Ethics Committee for Medical and Health Research at the Faculty of Medicine, Universitas Islam Indonesia, Yogyakarta, under approval number 24/Ka. Kom. Et/70/KE/VII/2023.

Extraction Process

In this study, the extraction process of pegagan leaf samples was carried out at the Pharmaceutical Biology Laboratory, Universitas Islam Indonesia, using 500 g of *C. asiatica* powder. The material was macerated with 96% ethanol at a ratio of 1:10 (w/v). The maceration was carried out at room temperature (25°C), protected from light with agitation. Each maceration step lasted for 24 hours, and the remaceration process was repeated three times with fresh solvent. The resulting extract was then filtered through Whatman filter paper using a vacuum Buchner funnel. The filtered liquid extract was concentrated by evaporation using a rotary evaporator until a thick ethanol extract was obtained. The yield of the thick extract was calculated as a percentage, and the extract was then placed in a vial and stored at 4°C in a refrigerator.

Preparation of Nanoemulsion C. asiatic Extract

The nanoemulsion formulation was developed by dissolving Pegagan extract in a mixture of 96% ethanol and propylene glycol within a 10 ml vial, followed by vortexing at 2500 rpm for 2 minutes. Subsequently, Tween 80 and distilled water were incorporated, and the mixture was further homogenized for 2 minutes. In the final step, isopropyl myristate was added and the formulation was homogenized using an ultrasonicator homogenizer (Model 150 VT) for 4 minutes. The optimized nanoemulsion formulation for the Pegagan extract consisted of 5% isopropyl myristate, 30% Tween 80, 15% ethanol, and 5% propylene glycol as presented in Table 1[17].

Formulation of nanohydrogel C. asiatic extract

The gel base utilized was carbopol 940. To prepare the gel base, carbopol 940 was dispersed in distilled water. The nanohydrogel of Pegagan extract was formulated by blending the prepared gel base with preservatives, specifically methyl paraben and propyl paraben. Glycerin, acting as a humectant, was then gradually incorporated until a homogeneous mixture was obtained. Following the uniform blending of the gel base, preservatives, and humectant, the Pegagan extract nanoemulsion was added. In the final step, TEA was introduced as a pH adjuster to achieve the desired pH and consistency as shown in the Table 2.

Evaluation of nanoemulsion matrix formulation

Organoleptic Test

Organoleptic test was conducted by evaluating the consistency, color, homogeneity, and odor of the Pegagan leaf extract nanoemulsion matrix[18].

Percentage transmittance

The percentage transmittance was measured using a UV-1800 Spectrophotometer. Prior to measurement, the optimal wavelength for the sample was determined within the range of 200-800 nm. The sample was diluted in distilled water at a ratio of 1:100[19].

Centrifugation Test

The sample was diluted 25 times with distilled water and placed into a microtube. It was then centrifuged for 30 minutes at 3000 rpm. The final step involved observing for any separation, sedimentation, creaming, or cracking[20].

Particle size, polydispersity index, and zeta potential test

The nanoemulsion matrix was stored at 40 ± 2°C for 3 months (high-temperature storage stability) and particle size, polydispersity index, and zeta potential of the Pegagan leaf extract nanoemulsion were assessed weekly using a Particle Size Analyzer (PSA). The obtained data were analyzed and interpreted[17].

Freeze Thaw Cycle Test

The nanoemulsion matrix was tested using the freeze-thaw cycle method, where the matrix was stored at 4 ± 2°C for 24 hours and then at room temperature for 24 hours (one cycle). This process was repeated for a total of 6 cycles. Subsequently, observations were made for changes in color, odor, and phase separation [21].

Transmission Electron Microscope (TEM)

The nanoemulsion sample was dropped onto a copper grid. Once it had dried completely, uranyl acetate was added and allowed to stain. The sample was then analyzed using a Transmission Electron Microscope (TEM), and the results were documented and interpreted[17].

Evaluation of nanohydrogel formulation
Organoleptic test

Organoleptic test was performed by evaluating the consistency, color, homogeneity, and odor of the Pegagan leaf extract nanohydrogel[19].

Power of Hydrogen (pH) Test

pH test was conducted by dissolving 0.5 g of the prepared nanohydrogel formulation in 50 mL of distilled water. The pH was then measured using a pH meter by immersing the electrode until a stable pH value was displayed on the screen. The target pH range for skin is 4.5–6.5. This test was performed with three repetitions[22].

Viscosity test

Viscosity was measured using a Brookfield viscometer DV-I Prime by immersing spindle No. 64 into the nanohydrogel formulation and recording the viscosity value displayed on the viscometer. This test was performed with three repetitions[22].

Spreadability test

0.5 g sample of the nanohydrogel was weighed and placed on a glass plate, then covered with a glass cover. A load of 150 g was applied and left for 1 minute. The diameter of the resulting gel spread was then measured[23].

Centrifugation test

10 g of the nanohydrogel sample were weighed and transferred into a conical tube. The tube was centrifuged for 30 minutes at 3000 rpm. The sample was then examined for any evidence of separation, sedimentation, creaming, or cracking[24].

Freeze thaw cycle test

The nanohydrogel formulation was subjected to stability testing using the freeze-thaw cycle method. The nanohydrogel was stored at 4 ± 2°C for 24 hours, followed by storage at room temperature for 24 hours (one cycle). This stability test was repeated for 3 to 6 cycles. Observations were then made for any changes in color, odor, and phase separation[21].

Wound healing activity in hyperglycemic rats
Acclimatization of experimental animals

The rats were acclimated for 1 week before the study to allow them adapt to the new environment and conditions. They were housed in designated cages, with 1 rat per cage, each cage measuring 40 cm x 30 cm x 10 cm, and fitted with sterilized wood shavings and wire mesh covers. The room conditions were kept at 24 ± 1°C with 55 ± 5% humidity and a 12-hour light/dark cycle. The rats were fed twice a day ad libitum (20 g per rat per day) and had access to distilled water via bottles. They were given AD 2 brand pellets as their diet[25].

Hyperglycemia induction

The rats were fasted for 6-8 hours prior to intraperitoneal induction using streptozotocin-nicotinamide. Streptozotocin (STZ) was freshly prepared in cold citrate buffer (0.1 M, pH 4.5) immediately prior to intraperitoneal injection to maintain its stability and biological activity. Initially, nicotinamide (230 mg/kg body weight) dissolved in 0.9% NaCl was administered. Streptozotocin (65 mg/kg) was given intraperitoneally 15 minutes after the administration of nicotinamide. Prior to injection, blood glucose levels were measured via the tail vein. Blood glucose levels were then monitored periodically on days 3, 7, and 17 post-induction. Rats with blood glucose levels >150 mg/dL (with a normal range of 50-135 mg/dL) were classified as diabetic and included in the study. Blood glucose levels were measured using an Accu-Chek glucometer[26,27]. The scheme for hyperglycemia induction is shown in Figure 1.

Excision wound model

The procedure for creating wounds in test animals involved shaving the fur from the area to be wounded one day before the procedure. Shaving was performed using an electric razor and the area was then cleaned with 70% ethanol. In the second stage, the animals were anesthetized with an intramuscular injection of ketamine (40:10 mg/kg). Subsequently, two excisional wounds, each with a diameter of 6 mm and spaced 1.5 cm apart, were created on each rat using a punch biopsy tool[25]. Figure 2 shows the schematic of the wound procedure in rats.

Application of nanohydrogel treatment on rats

The research subjects were allocated into 6 distinct groups as shown in Table 3.

Nanohydrogel was applied twice daily (morning and evening) by spreading it on the backs of the wounded rats according to the designated test groups. Observations were made on days 0 (the day of wounding), 5, 9, and 14, assessing macroscopic wound features such as redness, dryness, closure, and wound surface area using a caliper. At the end of the study, the rats were euthanized using CO2, and skin biopsies were performed for histopathological analysis[25,28]. The remains of the rats were incinerated by an external service.

Wound healing observation and measurement

Excisional wound observations on the rats were performed daily using macroscopic examination, while measurements were taken with a caliper on days 0, 5, 9, and 14. Figure 3 shows the schematic of wound healing activity.

Histopathological analysis

On day 14, tissue samples were excised. Initially, the rats were euthanized using CO2 inhalation, and samples were collected from the wound area. The tissues were fixed in 10% solution, then processed and sectioned into slices of 3–5 μm thickness using a microtome, followed by staining with hematoxylin and eosin. Collagen deposition in the healed tissue was assessed using Masson's Trichrome staining. Histological evaluation of the samples was performed to examine the changes induced by the nanohydrogel formulation[25,29].

Molecular docking study

The target receptors used in this study were selected based on previous research related to wound healing. These included Staphylococcus aureus tyrosyl-tRNA synthetase (PDB ID: 1JIJ, resolution: 3.20 Å)[30], mitogen-activated protein kinase 3 (MAPK3) (PDB ID: 2ZOQ, resolution: 2.39 Å), Nuclear Factor-κB (NF-κB) (PDB ID: 1SVC, resolution: 2.60 Å)[31], and the IL-6/IL-6Rα/IL-6Rβ complex (PDB ID: 1P9M, resolution: 3.65 Å)[32]. The 3D protein structures were downloaded from the RCSB Protein Data Bank (https://www.rcsb.org/), while the 3D structures of ligands, specifically asiatic acid, neomycin, and glutamic acid, were obtained from the PubChem database (https://pubchem.ncbi.nlm.nih.gov/). Protein preparation was conducted using PyMOL software version 3.0.5, and ligand preparation utilized Open Babel version 3.1.0. Docking evaluations were performed using PyRx version 0.8, which includes the AutoDock package. Visualization of docking results was carried out with Discovery Studio Visualizer version v24.1.0.23298.

Results and Discussion

Centella asiatic leaves extract

The extraction process of 500 grams of dried pegagan leaves yielded a thick extract that was dark green in color with a characteristic aroma, as determined by organoleptic evaluation. The weight of the thick extract obtained was 54.9745 grams, with a yield percentage of 10.99% (w/w). This result meets the minimum yield percentage requirement according to the Indonesian Herbal Pharmacopoeia II, which is not less than 7.3%. A higher yield percentage correlates directly with the amount of extract obtained during the extraction process[33]. The dried pegagan leaf sample (*Centella asiatica* (L.)) was extracted using the maceration method with 96% ethanol as the solvent (1:10 w/v)[34]. This method was chosen because asiaticoside, a compound in pegagan, is sensitive to heat, which could damage the chemical constituents of the leaves and affect the desired biological activity. Ethanol is reported to be effective in extracting saponins, flavonoids, tannins, alkaloids, and terpenoids[35].

Evaluation result of nanoemulsion matrix formulation

Organoleptic test

Based on the organoleptic evaluation, which assessed visual parameters including color, odor, and appearance, the nanoemulsion matrix base (without extract) and the nanoemulsion matrix of extracts Formula 1, Formula 2, and Formula 3 demonstrated stability after a 12-week stability test at elevated temperatures of 40±2ºC. There were no changes in appearance, color, or odor, as shown in Table 4.

Transmittance

The results of a 12-week (3-month) stability test at high temperature (40±2ºC) are presented in Table 5. The measurement of the percent transmittance aims to assess the clarity of the base nanoemulsion matrix (without extract) and the nanoemulsion matrix containing the *Centella asiatica* leaf extract. The percent transmittance is used as an initial basis for estimating the size of the nanoemulsion formulation. A good percent transmittance value ranges between 80-100%[19].

Based on the percent transmittance measurements, the Formula 1 nanoemulsion matrix exhibited a transmittance value of 89.507 ± 0.0 at

week 12. Given this result, the Formula 1 nanoemulsion matrix was selected as the nanoparticle carrier matrix for the active compound of *Centella asiatica* leaf extract. This choice is further supported by the lower surfactant composition percentage in Formula 1 compared to formulas Formula 2 and Formula 3. Other studies have reported that higher surfactant concentrations increase the potential for toxicity and irritation[36,37]. A higher transmittance value, closer to 100%, indicates that the nanoemulsion formed is transparent, which is an indication that the particle size falls within the nanometer range[38].

Centrifugation

The centrifugation test is a critical step to ensure the stability of a formulation against mechanical stress and gravitational forces. Smaller particle sizes enhance the ability to resist gravitational forces, thereby preventing phase separation in the formulation[39]. Based on the results of the centrifugation test, the nanoemulsion formulation was found to be stable, as evidenced by the absence of sedimentation, phase separation, creaming, and cracking.

Particle size, polydispersity index, and zeta potential test

Particle size analysis, Polydispersity Index (PI), and Zeta Potential are key parameters in the characterization of nanoemulsion formulations. The testing of these three parameters is conducted using a specialized instrument known as a particle size analyzer (PSA). The characterization results for the nanoemulsion matrix are presented in Table 5.

Based on the particle size analysis, there were no significant differences among the Formula 1, Formula 2, and Formula 3 nanoemulsion matrix after 12 weeks of testing. All three formulations met the nanoemulsion size acceptance criterion of ≤ 200 nm[17,34,39]. The purpose of particle size testing is to confirm that the formulation achieves a nanometer scale, which is related to its ability to deliver active ingredients more rapidly due to increased surface area and permeability in the nanoemulsion system[40,41].

The polydispersity index (PI) results showed that Formula 1 and Formula 2 met the acceptance criteria of ≤ 0.7. However, Formula 3 exhibited a PI value greater than 0.7 from week 8 to week 12. These results indicate that Formula 1 and Formula 2 remained stable after 12 weeks of testing. A PI value closer to zero indicates better stability, reflecting homogeneous and uniform particle sizes without aggregation[34,39,42].

The zeta potential measurement is crucial for assessing the stability of drug delivery systems that utilize nanoparticle technology. A nanoemulsion is considered stable if it meets the acceptance criterion of ≤ -30 mV[17,43]. According to the zeta potential data, the *Centella asiatica* extract nanoemulsions Formula 1 and Formula 2 were stable and met the acceptance criteria (≤ -30 mV) after 12 weeks of storage. However, the Formula 3 nanoemulsion did not meet the acceptance criterion from week 8 to week 12. The negative charge in the zeta potential value is likely due to the presence of fatty acids in the surfactant and cosurfactant, as well as sufficient repulsion between emulsion droplets, preventing coagulation and ensuring system stability[19].

Freeze thaw cycle

The results of the freeze-thaw test, conducted over 6 cycles, showed that both the base nanoemulsions (Formula 1, Formula 2, and Formula 3) and the *Centella asiatica* extract nanoemulsions (Formula 1, Formula 2, and Formula 3) passed the freeze-thaw cycle test. This is evidenced by the absence of changes in appearance, odor, or color, as well as the lack of phase separation, sedimentation, creaming, and cracking[44].

Transmission Electron Microscope (TEM)

The Transmission Electron Microscope (TEM) test aims to verify that the nanoemulsion formulation is formed with a size of ≤ 200 nm, is spherical in shape, and does not exhibit aggregation[45]. Based on TEM observations, as shown in Figure 4, the nanoemulsion globules are spherical and have a size of less than 50 nm.

Evaluation result of nanohydrogel formulation
Organoleptic

Based on the organoleptic testing conducted visually, which includes parameters of color, odor, and appearance, the base nanohydrogel (without extract) and the *Centella asiatica* extract nanohydrogels Formula 1, Formula 2, and Formula 3 were found to be stable after 12 weeks of stability testing at elevated temperatures of 40±2ºC. This stability is demonstrated by the absence of changes in form, color, and odor, as shown in Table 6.

Power of hydrogen (pH)

The pH test of the nanohydrogel formulations is conducted to ensure that the pH of the formulation is compatible with human skin. This is essential to minimize the risk of skin irritation that may arise from a mismatch between the formulation's pH and the skin's pH[46,47]. The results of the pH test are presented in Table 6.

The results from the 12-week testing indicate that the 1% base nanohydrogel, 1.5% base nanohydrogel, 1% extract nanohydrogel, and 1.5% extract nanohydrogel have all met the acceptance criteria for human skin pH, which is 4.5-6.5%[23].

Viscosity

According to the Indonesian National Standard (SNI 16-4380-1996), a good gel formulation should have a viscosity ranging from 3,000 to 50,000 cP. The viscosity evaluation of the nanohydrogel formulations, stored at elevated temperatures for 12 weeks, showed a decrease in

viscosity for both the base and extract nanohydrogels. However, this decrease remains within the acceptable range. The reduction in viscosity is attributed to environmental conditions[48]. The results of viscosity test are presented in Table 6.

Spreadability

The results shown in Table 6 indicate that the spreading ability of both the base nanohydrogel and the extract nanohydrogel ranges from 5 to 6.3 cm. These values fall within the acceptable range for good spreading ability, which is 5-7 cm[23,48].

Centrifugation

The centrifugation test is conducted to evaluate the impact of gravity on the stability of the nanohydrogel, simulating one year of gravitational stress. Based on the results of the 30-minute centrifugation test, the nanohydrogel formulations physically stable. This is evidenced by the absence of sedimentation, phase separation, creaming, and cracking[44].

Freeze thaw cycle

The results from the freeze-thaw testing (6 cycles) indicate that both the base nanohydrogels (Formula 1, Formula 2, and Formula 3) and the *Centella asiatica* extract nanohydrogels (Formula 1, Formula 2, and Formula 3) passed the freeze-thaw cycle test. This is demonstrated by the absence of changes in appearance, odor, and color, as well as no occurrence of phase separation, sedimentation, creaming, or cracking[44].

Hyperglycemia induction

The successful induction of hyperglycemia is essential as it is a prerequisite for advancing to subsequent research stages. Fasting blood glucose levels (FBGL) of the test animals were statistically analyzed to determine differences between pre- and post-induction with STZ-NA (streptozotocin-nicotinamide) at doses of 65 mg/kgBW and 230 mg/kgBW. The Shapiro-Wilk test was used to check for normal distribution of the data (Asymp. Sig (2-tailed) > α 0.05), followed by One-Way ANOVA to identify significant differences between groups. A Post-Hoc Tukey test was then applied to compare the average FBGL before and after induction. The results shown in Figure 5 indicate that the average FBGL of the animals on days 0, 3, 7, and 17 after induction displayed hyperglycemia (>150 mg/dL)[26], with significant differences ($p<0.05$). This significant difference confirms that the induction method was effective and valid, successfully causing hyperglycemia in the animals without resulting in mortality by the study's end.

These findings align with the theory that streptozotocin (STZ) induces hyperglycemia by destroying pancreatic beta cells. This process starts when STZ enters cells via the glucose-GLUT2 pathway, leading to DNA alkylation, which subsequently causes nitrate oxidation and activation of poly (ADP-ribose) polymerase[49,50]. The combination of streptozotocin and nicotinamide is used to reduce STZ toxicity, thereby decreasing the risk of animal death during the study[51].

Wound healing observation and measurement

Based on the results as shown in Table 7, it can be concluded that the positive control group achieved the highest wound healing percentage. The 1% and 1.5% nanohydrogel treatment groups followed, ranking second and third, respectively. A One-Way ANOVA was conducted to analyze the differences between the groups. The results of this statistical analysis, displayed as a graph showing the average wound healing percentage, are provided in Figure 5.

Based on the statistical analysis results on days 9 and 17 of the treatment, there were significant differences ($p<0.05$) between the negative control group and the positive control group, between the negative control group and the 1% nanohydrogel group, and between the negative control group and the 1.5% nanohydrogel group. These results indicate that the 1% and 1.5% nanohydrogel treatment groups with *Centella asiatica* extract had a significant effect compared to the negative control group (untreated) and are consistent with previous studies indicating that *Centella asiatica* has wound healing activity and that nanohydrogel formulations can enhance the effectiveness of wound healing[17,52,53]. Furthermore, the macroscopic parameters of wound healing are shown in Tables 8 and 9.

Macroscopic observations revealed no signs of infection or swelling in any of the test groups. The visual assessment parameters for dry wounds included the closure of the wound, the reduction, or even the absence of fluid around the wound, and the formation of scabs. A dry wound is an indication that the wound healing process has entered the hemostasis phase, which is the initial stage of wound healing where contraction occurs in the injured area, and bleeding stops as the blood clots and forms scabs. The coagulation process occurs due to platelet aggregation, which forms a fibrin network. This fibrin network serves as the foundation of the blood clot and as a temporary matrix for cell migration. Furthermore, platelets release cytokines and growth factors as proinflammatory signals to attract immune responses to the wound site[54]. Wound closure is characterized by the natural detachment of the scab, with the wound no longer being wet or bleeding after the scab has fallen off. Based on macroscopic observations, it was evident that the 1% nanohydrogel group accelerated the drying and closure of wounds more effectively compared to other groups, as shown in Figure 6.

Based on the wound healing effectiveness data, it was observed that nanohydrogel at a lower dosage provided better healing effects. This is likely

due to disruptions in the healing process, particularly during the inflammatory phase, and the high levels of Reactive Oxygen Species (ROS) generated by the higher dose of nanohydrogel. Other studies have reported that high concentrations of ROS during the wound healing process can inhibit healing and even cause tissue damage, extending to organ damage[55,56]. Additionally, elevated ROS levels lead to oxidative stress, which prolongs the inflammatory process by inducing macrophage and neutrophil chemotaxis and the expression of adhesion molecules in capillaries a condition commonly observed in chronic wounds. ROS play a role as intracellular signaling molecules to respond to extracellular stimuli. Moreover, ROS have been reported to contribute to the blood coagulation process through the mechanism of tissue factor (TF)-mRNA expression and the increased release of platelets and collagen formation. Therefore, a balanced amount of ROS is required to achieve cellular homeostasis, which is crucial for accelerating wound healing (Arief & Widodo, 2018). Furthermore, macroscopic observations on the nanohydrogel base showed the role of hydration in accelerating wound healing. The nanohydrogel base has the ability to maintain moisture, promote cell proliferation, and aid angiogenesis by delivering oxygen and nutrients to the wound bed, thus assisting in the healing of chronic wounds. This function can be enhanced by incorporating active substances, as seen in the 1% and 1.5% nanohydrogel groups[57,58].

Histopathological

Histopathological observations were conducted after a 14-day treatment period, involving skin tissue sampling from each group, which was then fixed using 10% formalin. Subsequent steps included preparing slides stained with Hematoxylin-Eosin (H&E) and Masson Trichrome (MT). H&E staining aimed to assess inflammation, while MT staining was used to evaluate the collagen composition in the skin tissue of each test group. The histopathological results are illustrated in Figures 7 and 8.

Based on the histopathological results, it was observed that the positive control, 1% nanohydrogel, and 1.5% nanohydrogel groups exhibited collagen composition at a moderate cellularity level compared to the normal group, while the negative control and base groups showed collagen composition at a low cellularity level. The MT staining results in the 1% and 1.5% nanohydrogel groups may be attributed to the role of interleukin-6 (IL-6), which aids in initiating fibroblast/keratinocyte profibrotic interactions. IL-6 induction in pro-inflammatory cytokine production in macrophages/monocytes occurs through the Mitogen-Activated Protein Kinases (MAPK) and Nuclear Factor-κB (NFκB) signaling pathways. This process is crucial for collagen formation during wound healing and its upregulation can promote recruitment of inflammatory cells such as neutrophils and macrophages, particularly during the early to intermediate stages of healing. Thus, the elevated inflammation observed in the 1% and 1.5% nanohydrogel groups may not indicate a pathological condition, but rather reflect an active and prolonged inflammatory phase, which is still part of the normal repair process.[59,60]. H&E staining results showed moderate inflammation in the positive and negative control groups, while severe inflammation was observed in the 1% and 1.5% nanohydrogel groups. The counts of lymphocytes, histiocytes, neutrophils, and giant cells are detailed in Table 10.

The cell count results indicated that the 1% and 1.5% nanohydrogel groups had a notable presence of histiocytes (macrophages), which are responsible for phagocytosing foreign substances in the tissue and clearing dead cells. The high number of histiocytes observed is consistent with the previous studies, which reported that they play a role in accelerating wound healing through increased production of collagenase enzymes. This is aligned with the MT staining results showing moderate levels of collagen in the 1% and 1.5% nanohydrogel groups[61–64]. Additionally, the 1% nanohydrogel group was rich in giant cells and lymphocytes compared to other groups. Conversely, high levels of neutrophils were observed in the negative, positive, nanohydrogel base, and 1.5% nanohydrogel groups compared to the 1% nanohydrogel group. Elevated neutrophil counts have been reported to potentially slow wound healing, as excessive neutrophil activity can increase tissue damage at the wound site, leading to prolonged inflammation, tissue damage, and ultimately delayed healing[61,62]. Other studies have indicated that a reduction in neutrophil counts can accelerate epithelialization without disrupting wound healing and collagen formation[62].

The lower neutrophil count observed in the 1% nanohydrogel group compared to the 1.5% group likely indicates that the 1% concentration provided a more optimal anti-inflammatory effect. At this dose, *Centella asiatica* may effectively suppress inflammation while supporting healing activities such as histiocyte and lymphocyte activation. In contrast, the 1.5% concentration did not result in a proportionally greater anti-inflammatory effect. Higher doses may trigger excessive inflammatory responses or local stress, potentially slowing the healing process. This suggests a dose-response relationship that is non-linear, with 1% appearing closer to the optimal therapeutic concentration.

One limitation of this study is the use of an animal model, which may not fully replicate the complexity of human skin physiology and wound healing mechanisms. Rodents heal primarily

through wound contraction, while humans rely more heavily on re-epithelialization, potentially limiting direct clinical translation of the results. Additionally, advanced molecular analyses such as gene expression profiling or protein quantification were not included. Future studies should consider validating the efficacy and safety of the Centella asiatica nanohydrogel in human skin models, such as ex vivo human skin or 3D skin equivalents. Clinical trials are also recommended to further explore its therapeutic potential and optimize the formulation for human use.

Molecular docking studies

In this study, asiatic acid was selected as the ligand for docking due to its presence in the nanohydrogel formulation of *Centella asiatica* extract. The docking analysis aimed to explore its activity with receptors associated with wound healing. Asiatic acid was chosen based on previous studies demonstrating its wound-healing properties[65–67]. Additionally, asiatic acid was compared with control ligands that promote wound healing, specifically neomycin and glutamic acid[68–70]. The docking results revealed that asiatic acid exhibited a stronger binding affinity than the controls. Comparative results of docking scores and amino acid residues for various target proteins are presented in Table 11.

The docking results shown in Figure 9 depict the 2D and 3D visual representations of asiatic acid and control ligands with various target proteins. The binding affinity of asiatic acid to the S. aureus protein, acting as an antibacterial agent, was -8.4 kcal/mol, which outperformed neomycin (control) with an affinity of -7.9 kcal/mol. Further analysis explored key molecular targets in wound healing: MAPK3, NF-κB, and IL-6. The binding affinities of asiatic acid with these three target proteins were -8.3, -6.9, and -8.5 kcal/mol, respectively. These values were superior to those of glutamic acid (control), which showed affinities of -4.6, -4.6, and -4.1 kcal/mol, respectively. These findings indicate that asiatic acid has the potential as a novel antibacterial agent, demonstrating significant activity in activating the MAPK pathway[70], suppressing inflammatory markers (NF-κB)[31], and upregulating the anti-inflammatory interleukin-6 (IL-6)[71].

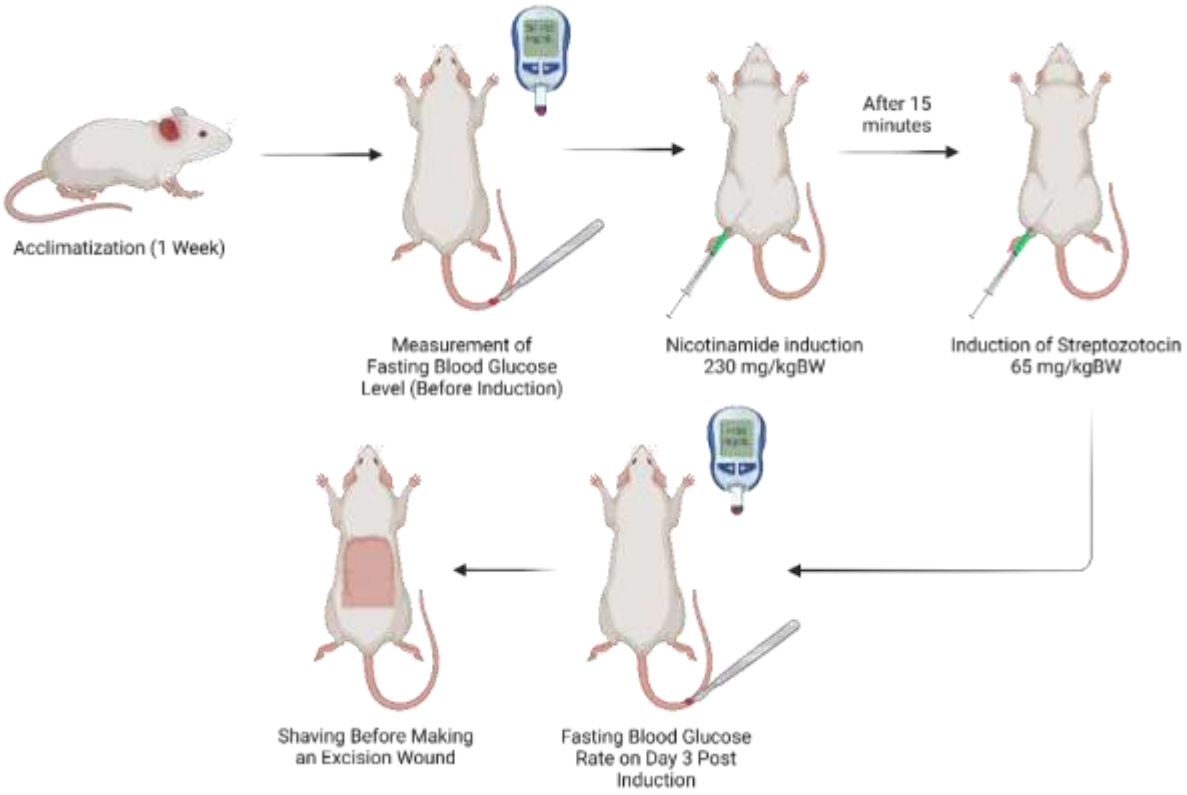

Figure 1. The schematic of hyperglycemia induction. Created with BioRender.com

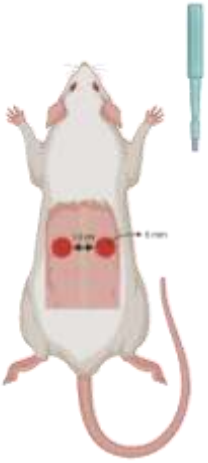

Figure 2. The schematic of the wound excision procedure in rats. Created with BioRender.com

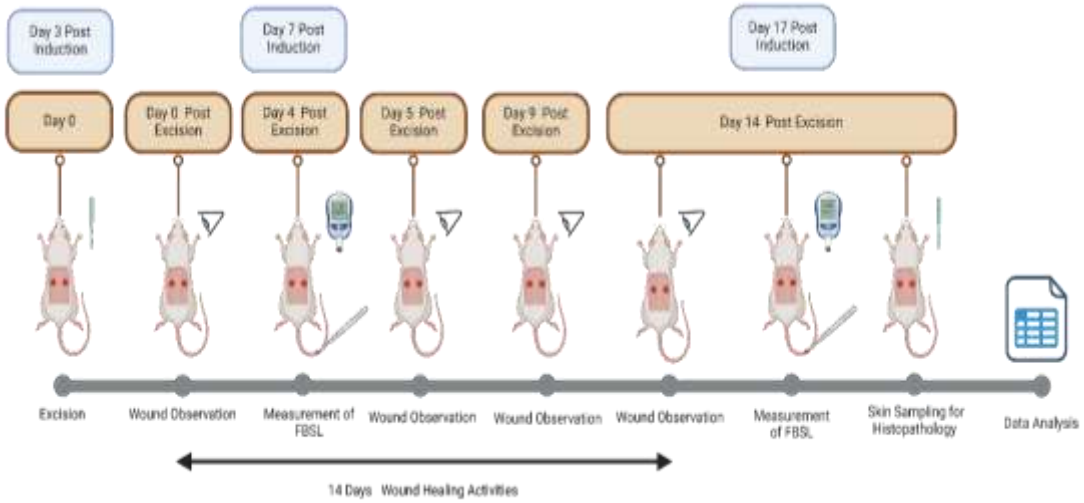

Figure 3. The schematic of Wound Healing Activity. Created with BioRender.com

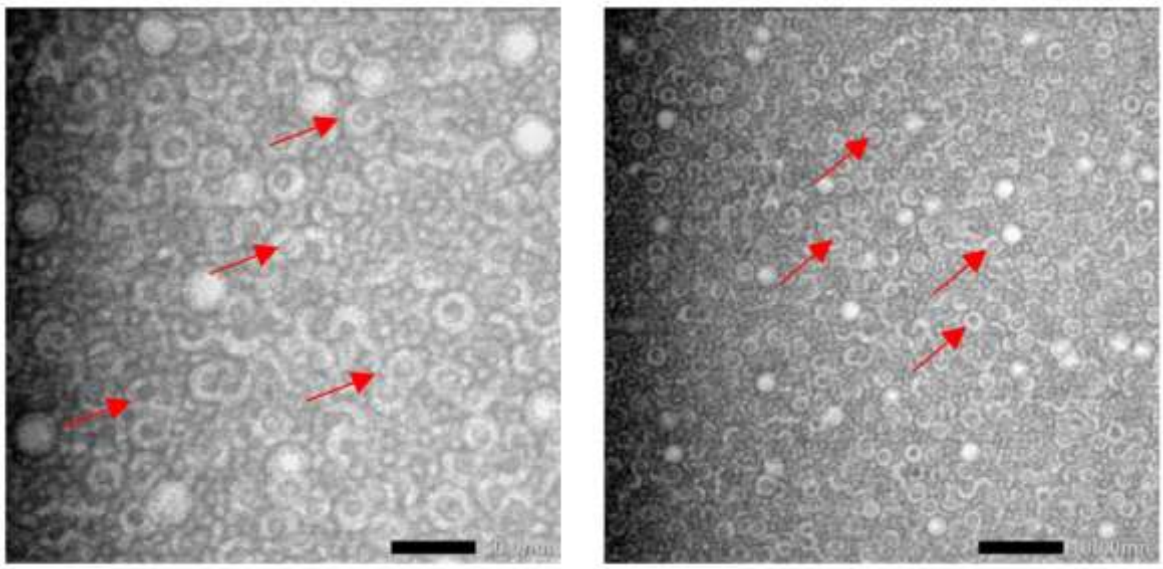

Figure 4. Transmission Electron Microscopy (TEM) Observation, (A) 50 nm Scale, (B) 100 nm

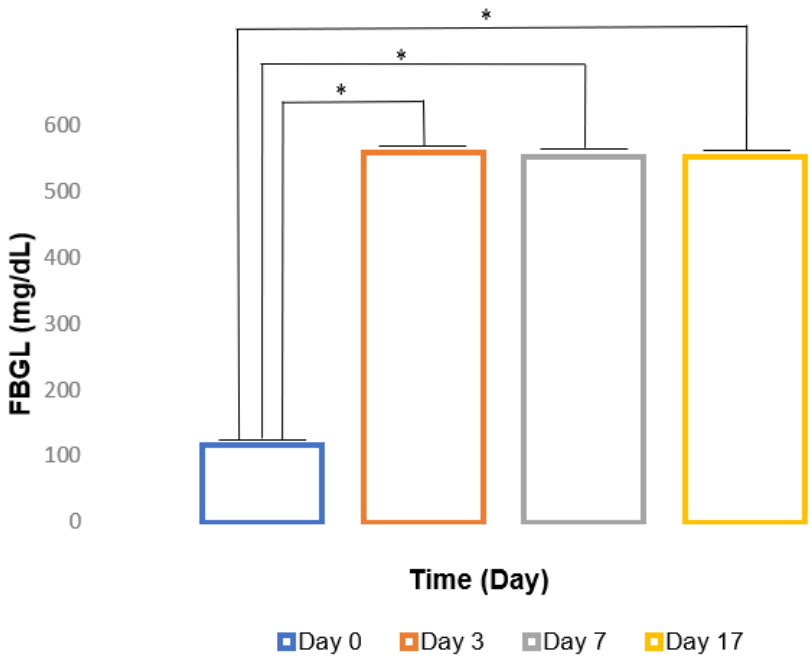

Figure 5. Graph of Average Glucose Levels of Experimental Animals (Pre and Post Induction)
Description: *Significant between pre and post ($p<0.05$)

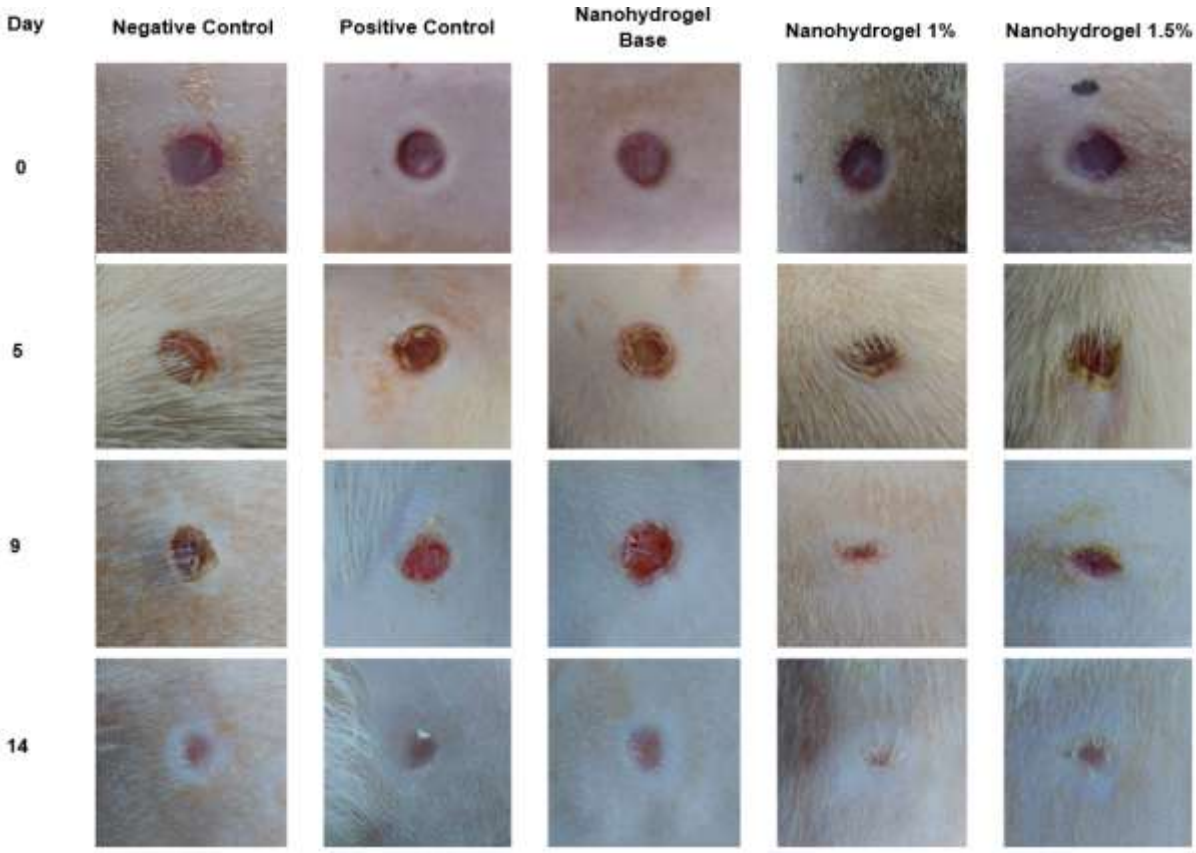

Figure 6. Macroscopic Observations of Excision Wounds

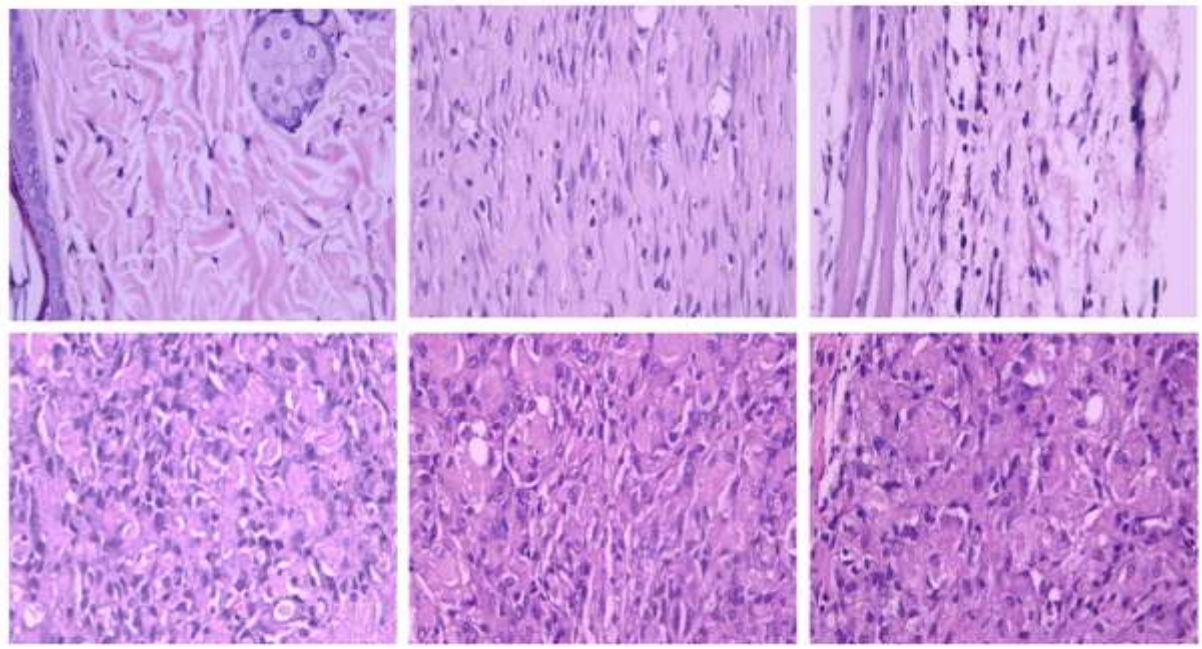

Figure 7. Histopathology Hematoxylin-Eosin Staining. Description: (A) Normal Control (Hyperglycemia induced without Excision), (B) Negative Control (Excision but no treatment), (C) Positive group (Excision and treated with Bioplacenton), (D) Base group (Excision and treated with nanohydrogel base), (E) Nanohydrogel 1% group (Excision and treated with 1% nanohydrogel), (F) Nanohydrogel 1.5% group (Excision and treated with 1.5% nanohydrogel).

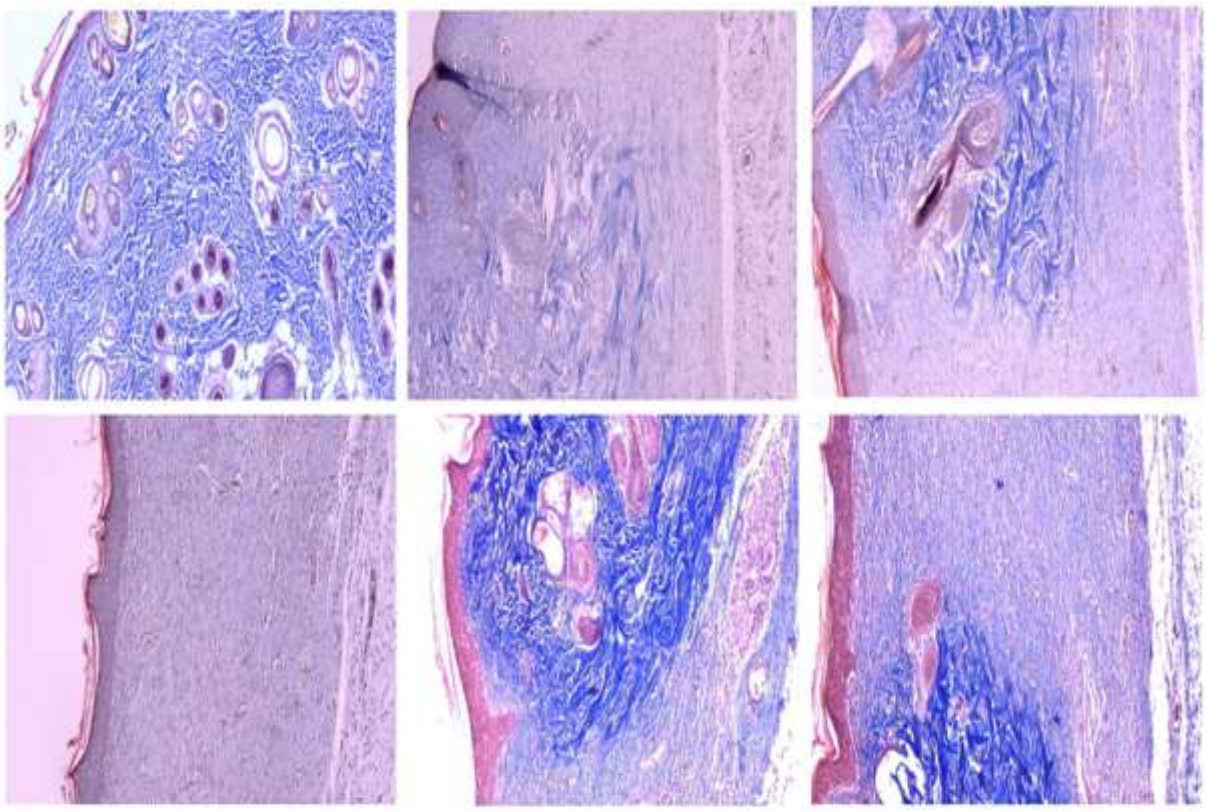

Figure 8. Histopathology Masson Trichrome Staining. Description: (A) Normal Control (Hyperglycemia induced without Excision), (B) Negative Control (Excision but no treatment), (C) Positive group (Excision and treated with Bioplacenton), (D) Base group (Excision and treated with nanohydrogel base), (E) Nanohydrogel 1% group (Excision and treated with 1% nanohydrogel), (F) Nanohydrogel 1.5% group (Excision and treated with 1.5% nanohydrogel)

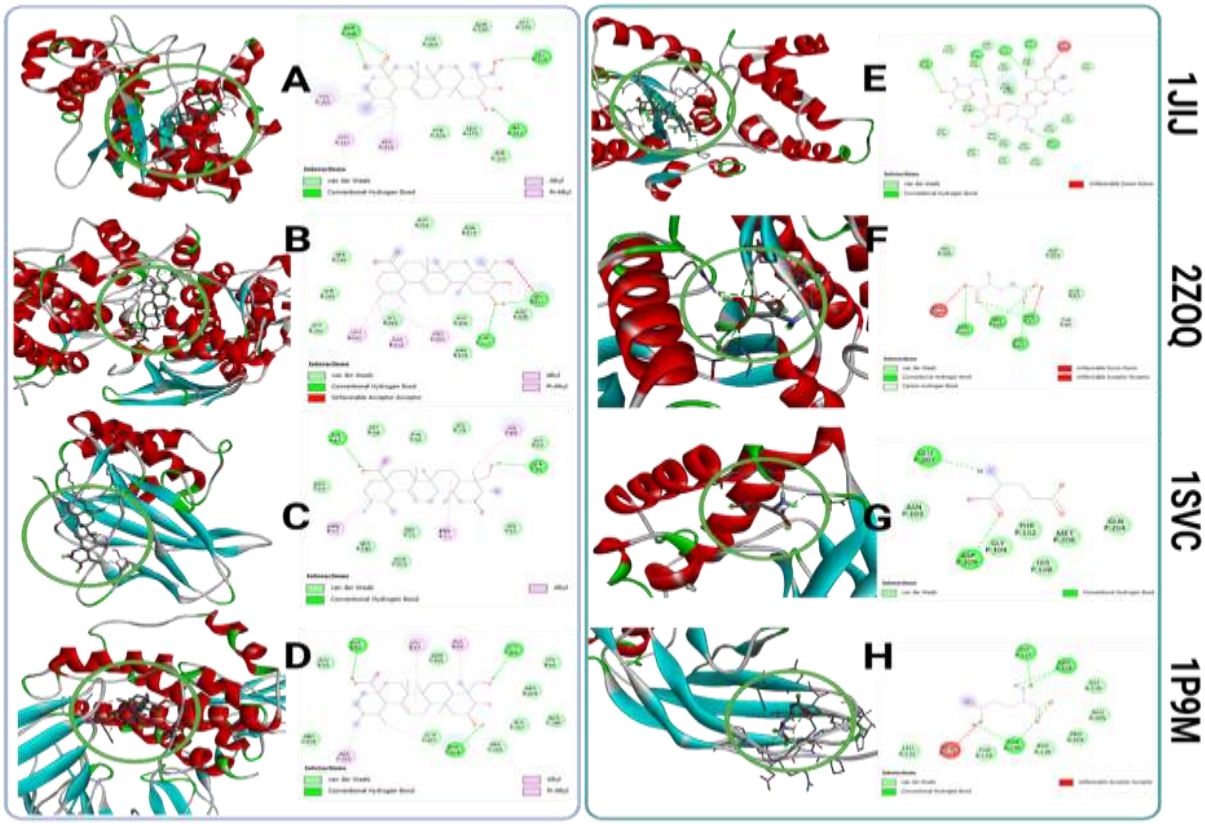

Figure 9. Two-dimensional and three-dimensional visualizations of the binding pose of asiatic acid (A-D), neomycin (E), and glutamic acid (F-G).

Table 1. Formulation of Nanoemulsion of *Centella asiatica* (L.) Extract

Matrix	Ingredients	Function	Formula 1 (%w/w)	Formula 2 (%w/w)	Formula 3 (%w/w)
Nanoemulsion Matrix	*Centella asiatica*	Active Substance	5	5	5
	Tween 80	Surfactant	30	35	40
	Isopropyl myristate	Oil Fase	5	5	5
	Propylene glycol	Cosurfactant	5	5	5
	Etanol 96%	Cosurfactant	15	15	15
	Aquadest	Solvent	ad 100	ad 100	ad 100

Table 2. Formulation of Nanohydrogel of *Centella asiatica* (L.) Extract

Matrix	Ingredients	Function	Formula 1 (%w/w)	Formula 2 (%w/w)
Nanoemulsion Matrix	Optimal Formula	Matrix for Active Ingredient Delivery	1%	1,5%
Gel base	*Carbopol 940*	*Gelling agent*	1	1
	Metil Paraben	Preservative	0.2	0.2
	Propil Paraben	Preservative	0.02	0.02
	Gliserin	Humectant	15	15
	TEA	*Adjustment* pH	qs	qs
	Aquades	Solvent	ad100	ad 100

Table 3. Treatment Group

Group	Description
Normal Control	Induction of hyperglycemia without any treatment
Negative Control	Induction of hyperglycemia and excision wounds without any treatment
Positive Control	Induction of hyperglycemia and excision wounds treated with povidone iodine

Continued 3

Nanohydrogel Base Control	Induction of hyperglycemia and excision wounds treated with nanohydrogel base control
Nanohydrogel 1% of *C. asiatica* Extract	Induction of hyperglycemia and excision wounds treated with nanohydrogel 1% of *C. asiatic* Extract
Nanohydrogel 1.5% of *C. asiatica* Extract	Induction of hyperglycemia and excision wounds treated with nanohydrogel 1.5% of *C. asiatic* Extract

Table 4. Organoleptic of Nanoemulsion

Dosage Form	Appearance	Color	Odor
Nanoemulsion Base Formula 1	Viscous Liquid	Clear Transparent	Distinctive Base
Nanoemulsion Base Formula 2	Viscous Liquid	Clear Transparent	Distinctive Base
Nanoemulsion Base Formula 3	Viscous Liquid	Clear Transparent	Distinctive Base
Nanoemulsion Extract Formula 1	Viscous Liquid	Dark Green	Distinct to *C. asiatica*
Nanoemulsion Extract Formula 2	Viscous Liquid	Dark Green	Distinct to *C. asiatica*
Nanoemulsion Extract Formula 3	Viscous Liquid	Dark Green	Distinct to *C. asiatica*

Description: Nanoemulsion Base: Nanoemulsion without *C. asiatica* Extract Nanoemulsion Extract: Nanoemulsion contained *C. asiatica* Extract

Table 5. Organoleptic of Nanoemulsion

Formula		**Week**	**Transmittance (%)**	**Particle Size (nm)**	***Polydispersity Index* (PI)**	**Zeta Potensial (mV)**
Formula 1	Nanoemulsion Base	Week 0	100.348±0.2	14.1 ± 0.6	0.196 ± 0.058	-36.5 ± 1.8
		Week 4	99.388±0.0	17.6 ± 0.3	0.521 ± 0.039	-32.3 ± 1.1
		Week 8	99.149 ± 0.0	17.5 ± 0.3	0.347 ± 0.205	-39.9 ± 0.2
		Week 12	99.393 ± 0,0	17.3 ± 0.4	0.283 ± 0.013	-34.4 ± 0.3
	Nanoemulsion Extract	Week 0	89.805±0.9	20.3 ± 0.3	0.242 ± 0.058	-37.4 ± 0.7
		Week 4	90.864±0.0	24.4 ± 0.7	0.299 ± 0.152	-31.5 ± 0.5
		Week 8	89.346 ± 0.0	24.3 ± 0.2	0.578 ± 0.026	-35.2 ± 1.0
		Week 12	89.507 ± 0.0	20.3 ± 0.3	0.414 ± 0.203	-31.0 ± 0.7
Formula 2	Nanoemulsion Base	Week 0	100.427±0.2	16.3 ± 0.6	0.184 ± 0.076	-34.3 ± 1.8
		Week 4	99.338±0.0	17.5 ± 0.4	0.366 ± 0.101	-38.5 ± 0.7
		Week 8	99.070 ± 0,0	18.0 ± 0.4	0.238 ± 0.155	-37.7 ± 0.3
		Week 12	98.330 ± 0.0	18.9 ± 0.1	0.252 ± 0.200	-32.7 ± 0.4
	Nanoemulsion Extract	Week 0	85.804±0.8	21.9 ± 0.3	0.610 ± 0.072	-35.0 ± 1.5
		Week 4	89.328±0.0	21.8 ± 0.1	0.311 ± 0.157	-31.7 ± 0.4
		Week 8	89.355 ± 0.0	24.4 ± 0.6	0.548 ± 0.048	-31.8 ± 0.9
		Week 12	89.036 ± 0.0	21.6 ± 1.0	0.492 ± 0.088	-31.4 ± 0.6
Formula 2	Nanoemulsion Base	Week 0	100.280±0.1	12.4 ± 1.0	0.393 ± 0.069	-33.4 ± 1.3
		Week 4	99.170±0.0	19.0 ± 0.3	0.338 ± 0.163	-38.9 ± 0.6
		Week 8	99.160 ± 0.0	16.1 ± 0.2	0.159 ± 0.024	-34.7 ± 0.1
		Week 12	98.645 ± 0.0	16.7 ± 0.9	0.501 ± 0.104	-34.0 ± 0.7
	Nanoemulsion Extract	Week 0	88.184±1.0	21.9 ± 0.3	0.521 ± 0.084	-35.8 ± 0.7
		Week 4	89.481±0.1	19.1 ± 0.7	0.514 ± 0.042	-32.0 ± 0.1
		Week 8	89.240 ± 0.0	30.3 ± 0.3	0.863 ± 0.029	-27.0 ± 0.6
		Week 12	89.067 ± 0.0	21.1 ± 0.2	0.914 ± 0.045	-22.0 ± 0.2

Description: Nanoemulsion Base: Nanoemulsion without *C. asiatica* Extract Nanoemulsion Extract: Nanoemulsion contained *C. asiatica* Extract

Table 6. Characterization Results of Nanohydrogel Over 12 Weeks (n=3)

Formula		Week	pH	Viscosity (cP)	Spreadibility
Formula 1	Nanohydrogel Base 1%	Week 0	4.9 ± 0.0	5117 ± 0.0	5.7 ± 0.0
		Week 4	4.8 ± 0.0	4241 ± 0.0	6.3 ± 0.0
		Week 8	4.8 ± 0.0	4007 ± 0.0	5.8 ± 0.0
		Week 12	4.6 ± 0.0	4013 ± 0.0	5.8 ± 0.0
	Nanohydrogel Extract 1%	Week 0	5.2 ± 0.0	5039 ± 0.0	5.0 ± 0.0
		Week 4	5.0 ± 0.0	4511 ± 0.0	6.2 ± 0.0
		Week 8	5.0 ± 0.0	4505 ± 0.0	5.7 ± 0.0
		Week 12	5.0 ± 0.0	4427 ± 0.0	5.5 ± 0.0
Formula 2	Nanohydrogel Base 1.5%	Week 0	5.0 ± 0.0	5951 ± 0.0	5.5 ± 0.0
		Week 4	4.9 ± 0.0	4865 ± 0.0	6.3 ± 0.0
		Week 8	4.8 ± 0.0	4487 ± 0.0	5.6 ± 0.0
		Week 12	4.7 ± 0.0	4487 ± 0.0	5.7 ± 0.0
	Nanohydrogel Extract 1.5%	Week 0	5.2 ± 0.0	4859 ± 0.0	5.0 ± 0.0
		Week 4	5.0 ± 0.0	4427 ± 0.0	5.8 ± 0.0
		Week 8	5.0 ± 0.0	4427 ± 0.0	5.8 ± 0.0
		Week 12	5.0 ± 0.0	4373 ± 0.0	5.3 ± 0.0

Description: Nanohydrogel Base: Nanohydrogel without *C. asiatica* Extract .Nanohydrogel Extract: Nanohydrogel contained *C. asiatica* Extract

Table 7. Wound Healing Percentage for Excision on the Back of Hyperglycemic Rats

Group	Day 0 (%)	Day 5 (%)	Day 9 (%)	Day 14 (%)
Negative	0±0	27.21±10.56	62.54±1.52	79.4±5.96
Positive	0±0	44.37±9.96	87.84±0.54	95.13±1.19
Nanohydrogel Extract 1%	0±0	25.06±10.64	62.72±1.20	79.88±5.71
Nanohydrogel Extract 1.5 %	0±0	41.07±16.18	85.81±0.70	92.47±2.64
Nanohydrogel Base	0±0	40.41±14.17	79.54±0.90	90.91±2.19

Description: Nanohydrogel Base: Nanohydrogel without *C. asiatica* Extract Nanohydrogel Extract: Nanohydrogel contained *C. asiatica* Extract

Table 8. Percentage of Dry Excision Wounds on the Back of Hyperglycemic Rats

Group	Dry Excision Wounds (%)			
	Day 0	Day 5	Day 9	Day 14
Negative	0	50.00	100	100
Positive	0	66.67	100	100
Nanohydrogel Extract 1%	0	83.33	100	100
Nanohydrogel Extract 1.5 %	0	66.67	100	100
Nanohydrogel Base	0	50.00	100	100

Description: Nanohydrogel Base: Nanohydrogel without *C. asiatica* Extract. Nanohydrogel Extract: Nanohydrogel contained *C. asiatica* Extract. The percentage of dry wounds is calculated by dividing the number of dry wounds by the total number of wounds in each group.

Table 9. Percentage of Clouser Excision Wounds on the Back of Hyperglycemic Rats

Group	Clouser Excision Wounds (%)			
	Day 0	Day 5	Day 9	Day 14
Negative	0	50.00	100	100
Positive	0	66.67	100	100
Nanohydrogel Extract 1%	0	83.33	100	100
Nanohydrogel Extract 1.5 %	0	66.67	100	100
Nanohydrogel Base	0	50.00	100	100

Description: Nanohydrogel Base: Nanohydrogel without *C. asiatica* Extract. Nanohydrogel Extract: Nanohydrogel contained *C. asiatica* Extract The percentage of clouser wounds is calculated by dividing the number of closed wounds by the total number of wounds in each group.

.

Table 10. Percentage of Clouser Excision Wounds on the Back of Hyperglycemic Rats

Group	Cell Type			
	Neutrophil	Giant Cell	Histiocyte	Lymphocyte
Negative	19	0	30	61
Positive	14	0	87	41
Nanohydrogel Extract 1%	5	11	778	81
Nanohydrogel Extract 1.5%	12	2	643	72
Nanohydrogel Base	12	1	179	82

Description: Nanohydrogel Base: Nanohydrogel without *C. asiatica* Extract. Nanohydrogel Extract: Nanohydrogel contained *C. asiatica* Extract The cell counts are based on observations at 400 x magnification and were conducted across 5 fields of view.

Table 11. Docking Scores and Hydrogen Bond Interactions of Asiatic Acid

Target	Protein	Interaction energy (kcal/mol)		Hydrogen Bond Interaction	
		Asiatic acid	Control	Asiatic acid	Control
Staphylococcus aureus tyrosyl-tRNA synthetase	1JIJ	-8.4	-7.9*	THR A:166, LEU A:128, ILE A:131	GLN A:196, ASP A:40, HIS A:50, HIS A: 47, PRO A:222*
MAPK3	2ZOQ	-8.3	-4.6**	THR B:312, LYS B:317	ARG B: 165, ARG B:189, ARG B: 84, ARG B: 87, **
NF-kb	1SVC	-6.9	-4.6**	HIS P:67, SER P:81	GLU P:207, ASP P:209**
IL-6/IL-6Rα/IL-6R beta (β) complex	1P9M	-8.5	-4.1**	ALA A:58, PHE C:134, SER C:166	THR A:130, GLY A:127, ARG A:128**

Conclusion

Nanohydrogel formulations of *Centella asiatica* leaf extract, specifically F1 (1%) and F2 (1.5%), were prepared using a nanoemulsion F1 matrix. The nanohydrogel met all acceptance criteria across various tests, including high-temperature storage, pH stability, spreadability, viscosity, centrifugation, and freeze-thaw cycles. Consequently, it can be concluded that the nanohydrogel formulation remains stable after 12 weeks of storage. In vivo efficacy evaluation of the nanohydrogel of *Centella asiatica* leaf extract on hyperglycemia-induced male Wistar rats demonstrated that the F1 (1%) nanohydrogel significantly accelerated wound healing. This conclusion was supported by macroscopic observations, wound healing percentage, histopathological analysis and molecular docking analysis.

Acknowledgment

We express our gratitude to the Department of Pharmacy, the Master of Pharmacy Study Program, and the Directorate of Research and Community Services at Universitas Islam Indonesia, as well as the Ministry of Education, Culture, Research, and Technology of the Republic of Indonesia, for providing support and facilities that enabled the completion of this research.

Conflicts of Interest

The authors assert that there are no conflicts of interest regarding this study.

Funding

Funding was provided by the Ministry of Education, Culture, Research, and Technology of the Republic of Indonesia through the Master's Thesis Research grants 2023, No. 0423.1/LL5-INT/AL.04/2023, and 017/ DirDPPM /70/DPPM/ PPS-PTM KEMDIKBUDRISTEK/VI/2023.

Ethics Statements

Ethical approval for this study was obtained from the Medical and Health Research Ethics Committee, Faculty of Medicine, Universitas Islam Indonesia, Yogyakarta, under approval number 24/Ka.Kom.Et/70/KE/VII/2023.

Author Contribution

Muhammad Hafizh Abiyyu Fathin Fawwazi, Writing–original draft, conceptualization, methodology, visualization, data curation, formal analysis; Farida Hayati and Lutfi Chabib, Conceptualization, funding acquisition, investigation, project administration, resources, supervision, validation; Tedi Rustandi, Writing-review and editing, visualization, software. All authors reviewed the results and approved the final version of the manuscript.

References

1. Magliano D, Boyko EJ. *IDF Diabetes Atlas*. 10th edition. Brussels: International Diabetes Federation; 2021. Accessed December 13, 2022. https:// diabetesatlas .org / atlas / tenth-edition /
2. Bekele F, Chelkeba L. Amputation rate of diabetic foot ulcer and associated factors in diabetes mellitus patients admitted to Nekemte referral hospital, western Ethiopia: prospective observational study. *J Foot Ankle Res* 2020;13(1):65. doi: 10.1186/s13047-020-00433 -9
3. Zhang CZ, Niu J, Chong YS, Huang YF, Chu Y, Xie SY, et al. Porous microspheres as promising vehicles for the topical delivery of poorly soluble asiaticoside accelerate wound healing and inhibit scar formation in vitro & in vivo. *Eur J Pharm Biopharm* 2016;109:1-13. doi: 10.1016/j.ejpb.2016.09.005
4. Frykberg RG, Banks J. Management of Diabetic Foot Ulcers: A Review. Published online 2016. doi: https:// doi. org/ 10. 12701 /jyms.2023.00682
5. Kasiya MM, Mang'anda GD, Heyes S, Kachapila R, Kaduya L, Chilamba J, et al. The challenge of diabetic foot care: Review of the literature and experience at Queen Elizabeth Central Hospital in Blantyre, Malawi. *Malawi Med J* 2017;29(2):218. doi: 10. 4314 /mmj .v29i2.26
6. Caruso P, Maiorino MI, Macera M, Signoriello G, Castellano L, Scappaticcio L, et al. Antibiotic resistance in diabetic foot infection: how it changed with COVID-19 pandemic in a tertiary care center. *Diabetes Res Clin Pract* 2021;175:108797. doi: 10.1016/ j.diabres .2021. 108797
7. Calixto JB. The role of natural products in modern drug discovery. *An Acad Bras Ciênc* 2019;91(suppl 3). doi: 10.1590/0001-376520 1920190105
8. Bansal K, Bhati H, Vanshita, Bajpai M. Recent insights into therapeutic potential and nanostructured carrier systems of Centella asiatica: An evidence-based review. *Pharmacol Res - Mod Chin Med* 2024;10:100403. doi: 10.1016/j.prmcm.2024.100403
9. Prakash V, Jaiswal N, Srivastava M. A Review on Medicinal Properties of Centella Asiatica. *Asian J Pharm Clin Res* 2017;10(10):69. doi: 10.22159/ajpcr.2017.v10i10.20760
10. Sutardi S. Kandungan Bahan Aktif Tanaman Pegagan dan Khasiatnya untuk Meningkatkan Sistem Imun Tubuh. *J Penelit Dan Pengemb Pertan* 2017;35(3):121. doi: 10.21082 /jp3. v35n3 . 2016.p121-130
11. Yuan Y, Zhang H, Sun F, Sun S, Zhu Z, Chai Y. Biopharmaceutical and pharmacokinetic characterization of asiatic acid in Centella asiatica as determined by a sensitive and robust HPLC–MS method. *J Ethnopharmacol* 2015; 163 : 31-8. doi: 10.1016/j.jep.2015.01.006
12. Shah S, Rangaraj N, Laxmikeshav K, Sampathi S. "Nanogels as drug carriers – Introduction, chemical aspects, release mechanisms and potential applications." *Int J Pharm* 2020 ;581 :119268. doi: 10.1016 /j. ijpharm. 2020.119268
13. Baskar V, I. SM, A. S, . S, Ali J, K. ST. Historic Review on Modern Herbal Nanogel Formulation and Delivery Methods. *Int J Pharm Pharm Sci* 2018;10(10):1. doi: 10.22159/ijpps.2018v10i10.23071
14. Chouhan D, Janani G, Chakraborty B, Nandi SK, Mandal BB. Functionalized PVA silk blended nanofibrous mats promote diabetic wound healing via regulation of extracellular matrix and tissue remodelling. *J Tissue Eng Regen Med* 2018;12(3). doi: 10.1002/term.2581
15. He W, Yao Z, Huang Y, Luo G, Wu J. A biological membrane-based novel excisional wound-splinting model in mice (With video). *Burns Trauma* 2014;2(4):196. doi: 10.4103/2321-3868.143625
16. Karina K, Biben JA, Ekaputri K, Rosadi I, Rosliana I, Afini I, et al. In vivo study of wound healing processes in Sprague-Dawley model using human mesenchymal stem cells and platelet-rich plasma. *Biomed Res Ther* 2021;8(4):4315-23. doi: 10.15419/bmrat.v8i4.670
17. Hanifah M, Jufri M. Formulation and Stability Testing of Nanoemulsion Lotion Containing Centella asiatica Extract. *J Young Pharm* 2018;10(4):404-8. doi: 10.5530/jyp.2018.10.89
18. Zanela Da Silva Marques T, Santos-Oliveira R, Betzler De Oliveira De Siqueira L, Da Silva Cardoso V, Maria Faria De Freitas Z, Barros RCSA, et al. Development and characterization of a nanoemulsion containing propranolol for topical delivery. *Int J Nanomedicine* 2018;Volume 13:2827-37. doi: 10.2147/IJN.S164404
19. Fitria A, Hanifah S, Chabib L, Uno AM, Munawwarah H, Atsil N, et al. Design and characterization of propolis extract loaded self-nano emulsifying drug delivery system as immunostimulant. *Saudi Pharm J* 2021;29(6):625-34. doi: 10.1016 /j. jsps. 2021 .04. 024
20. Nemade SM, Kakad SP, Kshirsagar SJ, Padole TR. Development of nanoemulsion of antiviral drug for brain targeting in the treatment of neuro-AIDS. *Beni-Suef Univ J Basic Appl Sci* 2022;11(1):138. doi: 10.1186/s43088-022-00319 -8
21. Agustin RD, Taihuttu YMJ. Formulation and physical stability test of hand sanitizer based on nutmeg oil (Myristica fragrans Houtt). *IOP Conf Ser Earth Environ Sci* 2021; 800 (1) :012032. doi: 10.1088/1755-1315/800/1/012032

22. Rahmawati DA, Setiawan I. The Formulation and Physical Stability Test Of Gel Fruit Strawberry Extract (Fragaria x ananassa Duch.). *J Nutraceuticals Herb Med* 2019;2(1):38-46. doi: https://doi.org/10.23917/jnhm.v2i1.8046

23. Nurman S, Yulia R, Irmayanti, Noor E, Candra Sunarti T. The Optimization of Gel Preparations Using the Active Compounds of Arabica Coffee Ground Nanoparticles. *Sci Pharm* 2019;87(4):32. doi: 10.3390/ scipharm 87040032

24. Dantas MGB, Reis SAGB, Damasceno CMD, Rolim LA, Rolim-Neto PJ, Carvalho FO, et al. Development and Evaluation of Stability of a Gel Formulation Containing the Monoterpene Borneol. *Sci World J* 2016;2016:1-4. doi: 10. 1155/2016/7394685

25. Alsareii SA, Ahmad J, Umar A, Ahmad MZ, Shaikh IA. Enhanced In Vivo Wound Healing Efficacy of a Novel Piperine-Containing Bioactive Hydrogel in Excision Wound Rat Model. *Molecules* 2023;28(2):545. doi: 10.3390/molecules28020545

26. Furman BL. Streptozotocin-induced diabetic models in mice and rats. *Curr Protoc* 2021;1(e78):1-21. doi: https:// doi. org/ 10. 1002/cpz1.78

27. Wolfensohn S, Lloyd M, editors. Small Laboratory Animals. In: *Handbook of Laboratory Animal Management and Welfare*. Oxford, UK: Blackwell Publishing Ltd; 2003. P. 233-71. doi: 10.1002/9780470751077.ch12

28. Hidayat R, Patricia Wulandari. Euthanasia Procedure of Animal Model in Biomedical Research. *Biosci Med J Biomed Transl Res* 2021;5(6):540-4. doi: 10.32539/bsm.v5i6.310

29. Algahtani MS, Ahmad MZ, Shaikh IA, Abdel-Wahab BA, Nourein IH, Ahmad J. Thymoquinone Loaded Topical Nanoemulgel for Wound Healing: Formulation Design and In-Vivo Evaluation. *Molecules* 2021;26(13):3863. doi: 10. 3390 /molecules 26133863

30. Sabarees G, Velmurugan V, Solomon VR. Molecular docking and molecular dynamics simulations discover curcumin analogs as potential wound healing agents. *Chem Phys Impact* 2024;8:100441. doi: 10. 1016 /j. chphi .2023.100441

31. el-dien RTM, Maher SA, Hisham M, Saber EA, Khedr AIM, Fouad MA, et al. Network pharmacology, molecular docking study, and in vivo validation of the wound healing activity of the Red Sea soft coral Paralemnalia thyrsoides (Ehrenberg 1834) ethanolic extract and bioactive metabolites. *Beni-Suef Univ J Basic Appl Sci* 2024;13(1):54. doi: 10.1186/s43088-024-00512-x

32. Groza Y, Lacina L, Kuchař M, Rašková Kafková L, Zachová K, Janoušková O, et al. Small protein blockers of human IL-6 receptor alpha inhibit proliferation and migration of cancer cells. *Cell Commun Signal* 2024;22(1):261. doi: 10. 1186/ s12964 - 024-01630 -w

33. Kementerian Kesehatan Republik Indonesia. *Farmakope Herbal Indonesia*. Edisi II.; 2017.

34. Hayati F, Salsabila T, Chabib L, Fawwazi MHAF. Self Nano Emulsifying Drug Delivery System (SNEDDS) Activity of Pegagan (Centella asiatica L) Extraction on Zebrafish Caudal Fins Regeneration. *J Res Pharm* 2022;26(7)(26(7)):1946-54. doi: 10. 29228 /jrp. 288

35. Harborne JB. *Metode Fitokimia Penuntun Cara Modern Mengenalisa Tumbuhan*. Bandung: ITB Press; 2006.

36. Bali V, Ali M, Ali J. Study of surfactant combinations and development of a novel nanoemulsion for minimising variations in bioavailability of ezetimibe. *Colloids Surf B Biointerfaces* 2010;76(2):410-20. doi: 10.1016 /j. colsurfb .2009.11.021

37. Yuan CL, Xu ZZ, Fan MX, Liu HY, Xie YH, Zhu T. Study on characteristics and harm of surfactants. Published online 2014.

38. Handoyo Sahumena M, Suryani S, Rahmadani N. Formulasi Self-Nanoemulsifiying Drug Delivery System (SNEDDS) Asam Mefenamat menggunakan VCO dengan Kombinasi Surfaktan Tween dan Span. *J Syifa Sci Clin Res* 2019;1(2):37-46. doi: 10.37311/jsscr.v1i2.2660

39. Jumaryatno P, Chabib L, Hayati F, Awaluddin R. Stability Study of Ipomoea reptans Extract Self-Nanoemulsifying Drug Delivery System (SNEDDS) as Anti-Diabetic Therapy. *J Appl Pharm Sci* 2018;8(9):11-4. doi: 10.7324 /JAPS. 2018. 8903

40. Algahtani MS, Ahmad MZ, Ahmad J. Nanoemulgel for Improved Topical Delivery of Retinyl Palmitate: Formulation Design and Stability Evaluation. *Nanomaterials* 2020; 10(5) :848 . doi: 10.3390/nano10050848

41. Donthi MR, Munnangi SR, Krishna KV, Saha RN, Singhvi G, Dubey SK. Nanoemulgel: A Novel Nano Carrier as a Tool for Topical Drug Delivery. *Pharmaceutics* 2023;15(1):164. doi: 10.3390/pharmaceutics15010164

42. Danaei M, Dehghankhold M, Ataei S, Hasanzadeh Davarani F, Javanmard R, Dokhani A, et al. Impact of Particle Size and Polydispersity Index on the Clinical Applications of Lipidic Nanocarrier Systems. *Pharmaceutics* 2018;10(2):57. doi: 10. 3390 /pharmaceutics 10020057

43. Singh Y, Meher JG, Raval K, Khan FA, Chaurasia M, Jain NK, et al. Nanoemulsion: Concepts, development and applications in drug delivery. *J Controlled Release* 2017;252:28-49. doi: 10.1016/j.jconrel.2017.03.008

44. Arianto A, Lie DYL, - S, Bangun HB. Preparation and Evaluation of Nanoemulgels

Containing a Combination of Grape Seed Oil and Anisotriazine as Sunscreen. *Open Access Maced J Med Sci* 2020;8(B):994-9. doi: 10. 3889 /oamjms.2020.5293

45. Aithal G, Nayak U, Mehta C, Narayan R, Gopalkrishna P, Pandiyan S, et al. Localized In Situ Nanoemulgel Drug Delivery System of Quercetin for Periodontitis: Development and Computational Simulations. *Molecules* 2018;23(6):1363. doi: 10.3390 /molecules 23061363

46. Paliwal S, Kaur G. Formulation and Characterization of Topical Nano Emulgel of Terbinafine. *Univers J Pharm Res* Published online January 11, 2019. doi: 10.22270 /ujpr .v3i6.223

47. Saryanti D, Zulfa IN. Optimization Carbopol And Glycerol As Basis Of Hand Gel Antiseptics Extract Ethanol Ceremai Leaf (Phyllantus Acidus (L.) Skeels) With Simplex Lattice Design. *JPSCR J Pharm Sci Clin Res* 2017;2(01):35. doi: 10.20961/jpscr.v2i01.5238

48. Yati K, Jufri M, Gozan M, Mardiastuti, Dwita LP. Pengaruh Variasi Konsentrasi Hidroxy Propyl Methyl Cellulose (HPMC) terhadap Stabilitas Fisik Gel Ekstrak Tembakau (Nicotiana tabaccum L.) dan Aktivitasnya terhadap Streptococcus mutans. *Pharm Sci Res* 2018;5(3). doi: 10.7454/psr.v5i3.4146

49. Raza H, John A. Streptozotocin-Induced Cytotoxicity, Oxidative Stress and Mitochondrial Dysfunction in Human Hepatoma HepG2 Cells. *Int J Mol Sci* 2012;13(5):5751-67. doi: 10.3390 /ijms 13055751

50. Tripathi V, Verma J. Different Models Used To Induce Diabetes: A Comprehensive Review. *Int J Pharm Pharm Sci* 2014;6(6).

51. Cruz PL, Moraes-Silva IC, Ribeiro AA, Machi JF, De Melo MDT, Dos Santos F, et al. Nicotinamide attenuates streptozotocin-induced diabetes complications and increases survival rate in rats: role of autonomic nervous system. *BMC Endocr Disord* 2021;21(1):133. doi: 10.1186/s12902-021-00795-6

52. Frida M, Mwangengwa L, Ally M. Excision wounds healing activity of Centella Asiatica (Gotukola) extract on laboratory rats. *Tanzan J Health Res* 2022;23(1). doi: https:// dx. doi. org /10.4314/thrb.v23i1.7

53. Morsy, Abdel-Latif, Nair, Venugopala, Ahmed, Elsewedy, et al. Preparation and Evaluation of Atorvastatin-Loaded Nanoemulgel on Wound-Healing Efficacy. *Pharmaceutics* 2019; 11 (11) :609. doi: 10.3390/ pharmaceutics 11110609

54. Alhajj M, Goyal A. *Physiology, Granulation Tissue*. StatePearls Publishing; 2022. Accessed March 28, 2024. https:// www. ncbi. nlm. nih. gov/books/NBK554402/

55. Arief H, Widodo MA. Peranan Stres Oksidatif pada Proses Penyembuhan Luka. *J Ilm Kedokt Wijaya Kusuma* 2018;5(2):22. doi: 10.30742 /jikw . v5i2.338

56. Ferreira CA, Ni D, Rosenkrans ZT, Cai W. Scavenging of reactive oxygen and nitrogen species with nanomaterials. *Nano Res* 2018;11(10):4955-84. doi: 10.1007/s12274-018-2092-y

57. Firlar I, Altunbek M, McCarthy C, Ramalingam M, Camci-Unal G. Functional Hydrogels for Treatment of Chronic Wounds. *Gels* 2022;8(2):127. doi: 10.3390/gels8020127

58. Gounden V, Singh M. Hydrogels and Wound Healing: Current and Future Prospects. *Gels* 2024;10(1):43. doi: 10.3390/gels10010043

59. Johnson BZ, Stevenson AW, Prêle CM, Fear MW, Wood FM. The Role of IL-6 in Skin Fibrosis and Cutaneous Wound Healing. *Biomedicines* 2020;8(5):101. doi: 10.3390/ biomedicines 8050101

60. Mathew-Steiner SS, Roy S, Sen CK. Collagen in Wound Healing. *Bioengineering* 2021;8(5):63. doi: 10.3390/ bioengineering 8050063

61. Konop M, Sulejczak D, Czuwara J, Kosson P, Misicka A, Lipkowski AW, et al. The role of allogenic keratin-derived dressing in wound healing in a mouse model. *Wound Repair Regen* 2017;25(1):62-74. doi: 10.1111/wrr.12500

62. Konop M, Czuwara J, Kłodzińska E, Laskowska AK, Zielenkiewicz U, Brzozowska I, et al. Development of a novel keratin dressing which accelerates full-thickness skin wound healing in diabetic mice: In vitro and in vivo studies. *J Biomater Appl* 2018;33(4):527-40. doi: 10.1177/0885328218801114

63. Konop M, Czuwara J, Kłodzińska E, Laskowska AK, Sulejczak D, Damps T, et al. Evaluation of keratin biomaterial containing silver nanoparticles as a potential wound dressing in full-thickness skin wound model in diabetic mice. *J Tissue Eng Regen Med* 2019;14(2):334-46. doi: 10.1002/term.2998

64. Kumar Reddy Sanapalli B, Tyagi R, Shaik AB, Pelluri R, Bhandare RR, Annadurai S, et al. L-Glutamic acid loaded collagen chitosan composite scaffold as regenerative medicine for the accelerated healing of diabetic wounds. *Arab J Chem* 2022;15(6):103841. doi: 10.1016/j.arabjc.2022.103841

65. Diniz LRL, Calado LL, Duarte ABS, De Sousa DP. Centella asiatica and Its Metabolite Asiatic Acid: Wound Healing Effects and Therapeutic Potential. *Metabolites* 2023;13(2):276. doi: 10.3390/metabo13020276

66. Mushtaq Z, Imran M, Hussain M, Saeed F, Imran A, Umar M, et al. Asiatic acid: a review on its polypharmacological properties and therapeutic potential against various Maladies. *Int J Food Prop* 2023;26(1):1244-63. doi: 10.1080/10942912.2023.2209702.

67. Witkowska K, Paczkowska-Walendowska M, Garbiec E, Cielecka-Piontek J. Topical Application of Centella asiatica in Wound Healing: Recent Insights into Mechanisms and Clinical Efficacy. *Pharmaceutics* 2024 ;16 (10) :1252. doi: 10.3390/ pharmaceutics16101252

68. Thangavel P, Ramachandran B, Chakraborty S, Kannan R, Lonchin S, Muthuvijayan V. Accelerated Healing of Diabetic Wounds Treated with L-Glutamic acid Loaded Hydrogels Through Enhanced Collagen Deposition and Angiogenesis: An In Vivo Study. *Sci Rep* 2017;7(1):10701. doi: 10.1038/ s41598 - 017-10882-1

69. Yang WT, Ke CY, Wu WT, Tseng YH, Lee RP. Antimicrobial and anti-inflammatory potential of Angelica dahurica and Rheum officinale extract accelerates wound healing in Staphylococcus aureus-infected wounds. *Sci Rep* 2020;10(1):5596. doi: 10.1038/s41598-020-62581-z

70. Chen Y, Zhang X, Wang Q, Du C, Dong CM. Wound microenvironment regulatory poly(L-glutamic acid) composite hydrogels containing metal ion-coordinated nanoparticles for effective hemostasis and wound healing. *Biomater Sci* 2024;12(5):1211-27. doi: 10. 1039 /d3bm01978k

71. Li Y, Zang J, Wang X, Feng X, Qiu F. Deciphering the underlying wound healing mechanisms of Streptocaulon juventas (Lour.) Merr. by integrating network pharmacology, transcriptomics, and experimental validation. *J Ethnopharmacol* 2023;302:115890. doi: 10. 1016 /j.jep.2022.115890

72. Bonnici L, Suleiman S, Schembri-Wismayer P, Cassar A. Targeting Signalling Pathways in Chronic Wound Healing. *Int J Mol Sci* 2023;25(1):50. doi: 10.3390/ijms25010050